Determination of Wave Noise Sources Using Spectral Parametric Modeling

Thierry Werling, *Student Member, IEEE,* Emmanuelle Bourdel, Daniel Pasquet, *Senior Member, IEEE,* and Ali Boudiaf

***Abstract*—A new method for the extraction of a noise correlation matrix is presented in this paper. This method is based on a kind of reflectometric technique which needs two noise-power measurements corresponding to two different input coefficients for the extraction of the wave correlation matrix. Then, we measure those two noise-power densities emanating from the device under test (DUT) transistor and compute their inverse Fourier transform (FT) in order to find out noise-power behaviors in time domain. Thus, one may apply spectral parametric modeling to this power spectral density (PSD) for the estimation of noise sources that model the DUT noisy two-port. Finally, we calculate the standard noise parameters of the transistor, and the results obtained by this new method are experimentally compared with a conventional method.**

***Index Terms*— Correlation matrix, noise figure, noise parameters, noise wave, power spectral density, spectral parametric modeling.**

I. Introduction

THE NOISE modeling of active devices requires the knowledge of four noise parameters [2]. These parameters are usually determined by different measurement techniques. The most commonly used is the source–pull tuner technique which requires an expensive bench (tuner), a large number of measurements with several source reflection coefficients, and a tuner calibration [6]. Faster methods are based on assumptions that depend either on the kind of transistor studied [MESFET or high electron-mobility transistor (HEMT)] [8]. Reflectometric methods are another way to extract a device under test (DUT) correlation matrix [5]. These methods are based on noise-wave representation [12], which is powerful in the microwave area. Nevertheless, the noise bench built for this method needs two circulators, hybrid couplers, and two different noise sources.

The new method proposed in this paper is derived from reflectometric method. It is based on the analysis of the wave power density in the time domain, which is obtained by an inverse Fourier transform (FT) of the measured noise power. Thus, we obtain the noise-power distribution in the time domain called wave-signal autocorrelation. This point of view allows the use of spectral estimators (parametric models) like the autoregressive (AR) model [1], [7], [9]. Aside from that, this new method enables us to determine the exact DUT reference plane and allows the S_{11}-parameter extraction.

Manuscript received March 31, 1997; revised August 1, 1997.

T. Werling, E. Bourdel, and D. Pasquet are with the Ecole Nationale Supérieure de l'Electronique et de ses Applications (ENSEA-EMO), 95014 Cergy Cedex, France (e-mail: werling@ensea.fr; pasquet@ensea.fr; bourdel@ensea.fr; boudiaf@univ-mlv.fr).

A. Boudiaf is with the Universite Marne la Vallée, Noisy-le Grand Cedex, France.

Publisher Item Identifier S 0018-9480(97)08340-3.

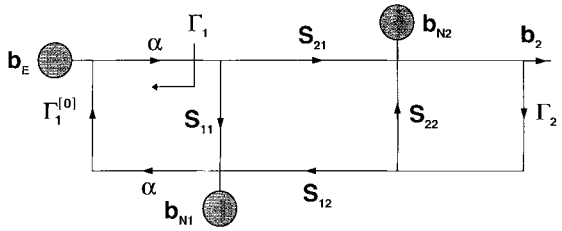

Fig. 1. The representation of a two-port circuit element using scattering parameters and noise waves.

II. The Noise-Wave Representation

This kind of representation is very helpful for the microwave-domain analysis. In the noise-wave representation, the noise of a circuit element is described by using waves that emanate from its ports. A linear two-port, represented by noise wave and scattering parameters, is shown in Fig. 1. Noise waves b_{N1} and b_{N2} contribute to the scattered waves. Thus, the wave variables and scattering parameters satisfy the following:

$$\begin{pmatrix} b_1 \\ b_2 \end{pmatrix} = \begin{pmatrix} S_{11} & S_{12} \\ S_{21} & S_{22} \end{pmatrix} \cdot \begin{pmatrix} a_1 \\ a_2 \end{pmatrix} + \begin{pmatrix} b_{\mathrm{N1}} \\ b_{\mathrm{N2}} \end{pmatrix}. \tag{1}$$

The noise waves are time-varying complex random variables characterized by a correlation matrix given by [4] as follows:

$$C_S = \begin{pmatrix} \langle |b_{N1}|^2 \rangle & \langle b_{\mathrm{N1}} b_{\mathrm{N2}}^* \rangle \\ \langle b_{\mathrm{N1}}^* b_{\mathrm{N2}} \rangle & \langle |b_{\mathrm{N2}}|^2 \rangle \end{pmatrix} = \begin{pmatrix} \langle |b_{\mathrm{N1}}|^2 \rangle & CS_{21}^* \\ C^* S_{21} & \langle |b_{\mathrm{N2}}|^2 \rangle \end{pmatrix} \tag{2}$$

where $\langle . \rangle$ indicates time averaging with an implicit assumption of ergodicity and jointly wide-sense stationary processes. The diagonal terms of C_S give the noise power deliverable to the terminations in a 1-Hz bandwidth, and the off-diagonal terms are correlation products. All noise power are normalized with regard to the kT_0 factor where k is the Boltzmann constant and T_0 is equal to 290 K.

The output noise power (Fig. 1) is equal to $\langle |b_2|^2 \rangle$ and its expression is given in (3), shown at the bottom of the following page. Equation (3) is the noise-power expression on which the new method is based for noise correlation matrix extraction.

III. Noise-Receiver Modeling

The RF signal emanating from the DUT is amplified through a 20-dB low-noise amplifier (see Fig. 2). Then, the amplified

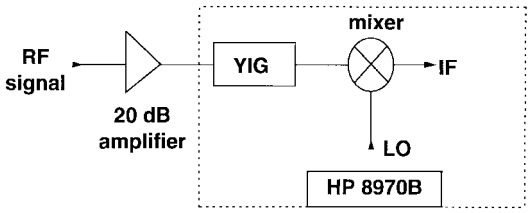

Fig. 2. The schematic representation of the NR.

signal is measured by the HP 8970B noise-figure meter (noise-power measurement mode) in single sideband. For this noise receiver (NR) the standard noise parameters [4], [5] can be simplified with the assumption of uncorrelated noise-wave sources. Our study has proven that the $\langle|b_{\rm N1}^{\rm NR}|^2\rangle$ effect can be neglected. Thus

$$r_n^{\rm NR} \approx \frac{1}{4}\cdot\left\langle\left|\frac{b_{\rm N2}^{\rm NR}}{S_{21}^{\rm NR}}\right|^2\right\rangle\cdot|1+S_{11}^{\rm NR}|^2 \tag{4}$$

$$F_{\rm min}^{\rm NR} \approx 1+\left\langle\left|\frac{b_{\rm N2}^{\rm NR}}{S_{21}^{\rm NR}}\right|^2\right\rangle\cdot\left[1-|S_{11}^{\rm NR}|^2\right] \tag{5}$$

$$\Gamma_{\rm opt}^{\rm NR} \approx S_{11}^{\rm NR^*} \tag{6}$$

with

$$F_0^{\rm NR} = 1+\left\langle\left|\frac{b_{\rm N2}^{\rm NR}}{S_{21}^{\rm NR}}\right|^2\right\rangle \tag{7}$$

are expressions for the four noise parameters where $F_0^{\rm NR}$ is the noise factor under matched input impedance ($|\Gamma_1| = 0$). Equation (6) agrees with studies made by using conventional methods [6].

IV. Theory

We have studied the output noise-wave behaviors of several transistors such as MESFET's and HEMT's and, in this case, the $\langle|b_2|^2\rangle$ expression in (3) is simplified, as shown in (8), at the bottom of the page.

After a usual calibration, two noise-power measurements with different input reflection coefficients ($|\Gamma_1|$ around 0.8 and $|\Gamma_1|$ close to zero) are necessary to separate the two terms that compose (8) and are shown in (9), at the bottom of the page, and

$$\left\langle\left|\frac{b_{\rm N2}}{S_{21}}\right|^2\right\rangle \tag{10}$$

can be developed in order to make the electrical length between Γ_1 and S_{11} appear. Indeed, the load coefficient reflection (see Fig. 1) is supposed to be

$$\Gamma_1 = \Gamma_1^{[0]}\alpha^2 e^{-j2\pi f\tau} = |\Gamma_1^{[0]}|\alpha^2 e^{-j2\pi f\tau+\Phi}. \tag{11}$$

Equation (9), with knowledge of (11), leads to (12), as shown at the bottom of the page, where γ_y is called the y-signal power spectral density (PSD) The PSD totally describes behaviors of stationary Gaussian processes. Equation (12) may be expressed as

$$\gamma_y(f) = \frac{\alpha(f)+2\beta(f)\cos\left[2\pi f\tau-\Phi_\beta(f)\right]}{|1-\rho(f)e^{-j2\pi f\tau}|^2} \tag{13}$$

where $\alpha(f)$, $\beta(f)$, $\Phi_\beta(f)$, and $\rho(f)$ are defined by

$$\alpha(f) = \langle|b_E|^2\rangle + |\Gamma_1|^2[\langle|b_{\rm N1}|^2\rangle - 2|S_{11}C|\cos(\Phi_{S_{11}}-\Phi_C)] \tag{14}$$

$$\beta(f) = |\Gamma_1 C| \tag{15}$$

$$\Phi_\beta(f) = \Phi+\Phi_C \tag{16}$$

$$\rho(f) = \Gamma_1^{[0]}\alpha^2 S_{11}. \tag{17}$$

Equation (13) may be written as follows in order to apply spectral modeling such as AR and moving average (MA)

$$\frac{\langle|b_2|^2\rangle}{|S_{21}|^2} = \frac{\langle|b_E|^2\rangle+|\Gamma_1|^2\langle|b_{\rm N1}|^2\rangle+2\,{\rm Re}\left[\Gamma_1(1-\Gamma_1S_{11})^*\left\langle b_{\rm N1}\left(\frac{b_{\rm N2}}{S_{21}}\right)^*\right\rangle\right]+|1-\Gamma_1S_{11}|^2\left\langle\left|\frac{b_{\rm N2}}{S_{21}}\right|^2\right\rangle}{|(1-\Gamma_1S_{11})(1-\Gamma_2S_{22})-\Gamma_1\Gamma_2S_{12}S_{21}|^2} \tag{3}$$

$$\frac{\langle|b_2|^2\rangle}{|S_{21}|^2} = \frac{\langle|b_E|^2\rangle+|\Gamma_1|^2\langle|b_{\rm N1}|^2\rangle-2|\Gamma_1|^2\,{\rm Re}\,(S_{11}^*C)+2\,{\rm Re}\,(\Gamma_1C)}{|1-\Gamma_1S_{11}|^2}+\left\langle\left|\frac{b_{\rm N2}}{S_{21}}\right|^2\right\rangle \tag{8}$$

$$\gamma_y(f) = \frac{\langle|b_E|^2\rangle+|\Gamma_1|^2\langle|b_{\rm N1}|^2\rangle-2|\Gamma_1|^2\,{\rm Re}\,(S_{11}^*C)+2\,{\rm Re}\,(\Gamma_1C)}{|1-\Gamma_1S_{11}|^2} \tag{9}$$

$$\gamma_y(f) = \frac{\langle|b_E|^2\rangle+|\Gamma_1|^2[\langle|b_{\rm N1}|^2\rangle-2|S_{11}C|\cos(\Phi_{S_{11}}-\Phi_C)]+2|\Gamma_1C|\cos(2\pi f\tau-\Phi-\Phi_C)}{|1-\Gamma_1^{[0]}\alpha^2S_{11}e^{-j2\pi f\tau}|^2} \tag{12}$$

Reduced Frequency ν	Frequency f_i
0	f_{min}
k/N	$f_{min} + kf_{step}$
(N-1)/N	f_{max}

Fig. 3. Relation between reduced frequency and measurement frequency.

modeling [11]:

$$\gamma_y(f) = \gamma_x(f)\left|\frac{1+\rho_b(f)e^{-j2\pi f\tau}}{1+\rho_a(f)e^{-j2\pi f\tau}}\right|^2 = \gamma_x(f)|h(f)|^2. \quad (18)$$

Thus, identification between (14)–(17) and (18) leads to the following equations:

$$\alpha(f) = \gamma_x(f)[1+|\rho_b(f)|^2] \quad (19)$$

$$\beta(f) = \gamma_x(f)|\rho_b(f)| \quad (20)$$

$$\Phi_\beta(f) = \arg[\rho_b(f)] \quad (21)$$

$$\rho(f) = -\rho_a(f). \quad (22)$$

Then we compute inverse FT in order to obtain y and b_{N2} autocorrelation sequences.

With $N\,\gamma_y$ data, each element of autocorrelation sequence [1], [7] is calculated by

$$C_y[k] = \frac{1}{N}\sum_{i=0}^{N-1}\gamma_y(f_i)e^{-j2\pi(ik/N)}, \qquad \text{with } 0 \le k \le N-1 \quad (23)$$

where f_i is the frequency that belongs to the frequency-range measurement $[f_{\min}, f_{\max}]$. The AR modeling is a parametric PSD modeling under the assumption of signal Gaussianity [7]. Before explaining AR modeling, let us introduce the reduced-frequency variable ν. Fig. 3 gives equivalence between the measurement frequency and the reduced frequency where ν verifies

$$\nu \in \left[0, \cdots, \frac{i}{N}, \cdots, \frac{N-1}{N}\right]. \quad (24)$$

We may introduce the parameter U that corresponds to the time parameter τ (see Fig. 4) so that in discrete frequency domain, (18) leads to

$$\gamma_y(\nu) = \gamma_x(\nu)\left|\frac{1+\rho_b(\nu)e^{-j2\pi\nu U}}{1+\rho_a(\nu)e^{-j2\pi\nu U}}\right|^2 = \gamma_x(\nu)|h(\nu)|^2 \quad (25)$$

where

$$h(\nu) = \frac{1+\rho_b(\nu)e^{-j2\pi\nu U}}{1+\rho_a(\nu)e^{-j2\pi\nu U}}. \quad (26)$$

An AR modeling is used in order to estimate the $[\gamma_x(\nu), \rho_a(\nu), \rho_b(\nu)]$ parameters which appear in (25). The AR modeling decomposes the y-signal PSD in the following way:

$$\gamma_y(\nu) = \frac{\sigma^2_{\mathrm{AR}}}{\left|1+\sum_{i=1}^{P_L} c_i e^{-j2\pi\nu i}\right|^2} \quad (27)$$

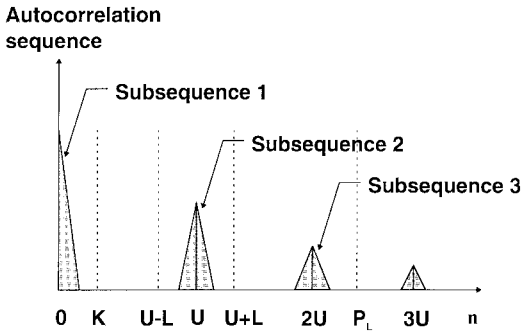

Fig. 4. y-signal autocorrelation sequence.

where $(\sigma^2_{\mathrm{AR}}, c_1, \cdots, c_{P_L})$ are called AR parameters and P_L+1 the AR order. AR parameters are extracted by solving (28), called the Yule–Walker equations. It is done by using the Levinson's recursive algorithm [13]:

$$\begin{bmatrix} C_y[0] & C_y[1] & \cdots & C_y[P_L] \\ C_y[1] & C_y[0] & \cdots & C_y[P_L-1] \\ C_y[2] & C_y[1] & \cdots & C_y[P_L-2] \\ \vdots & \vdots & \vdots & \vdots \\ C_y[P] & C_y[P-1] & \cdots & C_y[0] \end{bmatrix} \cdot \begin{bmatrix} 1 \\ c_1 \\ c_2 \\ \vdots \\ c_{P_L} \end{bmatrix} = \begin{bmatrix} \sigma^2_{\mathrm{AR}} \\ 0 \\ 0 \\ \vdots \\ 0 \end{bmatrix}. \quad (28)$$

On the one hand, the x-signal PSD may be estimated by setting c_i coefficients to zero for $i > K$ in (27) (see Fig. 4):

$$\gamma_x(\nu) = \frac{\sigma^2_{\mathrm{AR}}}{\left|1+\sum_{i=1}^{K} c_i e^{-j2\pi\nu i}\right|^2}. \quad (29)$$

On the other hand, one may obtain the $|h(\nu)|^2$ function by dividing (27) by (28) [see (25)]:

$$|h(\nu)|^2 = \left|\frac{1+\rho_b(\nu)e^{-j2\pi\nu U}}{1+\rho_a(\nu)e^{-j2\pi\nu U}}\right|^2. \quad (30)$$

Finally, $\rho_a(\nu)$ and $\rho_b(\nu)$ coefficients are developed with discrete FT (DFT):

$$\rho_a(\nu) = \sum_{i=-L}^{L}\rho_{a_i}e^{-j2\pi\nu i} \quad (31)$$

$$\rho_b(\nu) = \sum_{i=-L}^{L}\rho_{b_i}e^{-j2\pi\nu i} \quad (32)$$

reporting (31) and (32) into (26) leads to

$$h(\nu) = \frac{1+\sum_{i=-L}^{L}\rho_{b_i}e^{-j2\pi\nu(U+i)}}{1+\sum_{i=-L}^{L}\rho_{a_i}e^{-j2\pi\nu(U+i)}}. \quad (33)$$

This frequency response is analyzed with an AR MA (ARMA) modeling in order to estimate ρ_{a_i} and ρ_{b_i} coefficients. The ARMA frequency response is defined by

$$h_{\mathrm{ARMA}}(\nu) = \frac{1 + \sum_{q=1}^{Q} b_q e^{-j2\pi\nu q}}{1 + \sum_{p=1}^{P} a_p e^{-j2\pi\nu p}} \tag{34}$$

where b_q are the MA coefficients and a_p the AR coefficients of this function. Identification between (32) and (33) yields

$$\rho_{b_i} = b_{U+i} \tag{35}$$

$$\rho_{a_i} = a_{U+i} \tag{36}$$

where i verifies $-L \le i \le L$. Other a_i and b_i values are supposed to be null, except $a_0 = 1$ and $b_0 = 1$.

The a_i and b_i coefficients are related to c_i coefficients through

$$\left(1 + \sum_{i=K+1}^{P_L} c_i e^{-j2\pi\nu i}\right)\left(1 + \sum_{q=1}^{Q} c_i e^{-j2\pi\nu q}\right) = 1 + \sum_{p=1}^{P} c_i e^{-j2\pi\nu p}. \tag{37}$$

Equation (36) leads to the following:

$$\sum_{k=0}^{Q} b_k c_{n-k} = a_n, \qquad \text{for } n \ge 0 \tag{38}$$

$$\sum_{k=0}^{Q} b_k c_{n-k} = 0, \qquad \text{for } n \ge P. \tag{39}$$

Aside from this, $b_0 = 1$ and b_k coefficients are null for $k = 1$ to $k = U - L - 1$ and $k = U + L + 1$ to Q so that (39) yields

$$\sum_{k=U-L}^{U+L} b_k c_{n-k} = -c_n, \qquad \text{for } n \ge U + L. \tag{40}$$

Equation (40) yields the matrix equation in (41), built by setting different values for n ($n \in [2U - L, 2U + L]$):

$$\begin{pmatrix} c_U & c_{U-1} & c_{U-2} & \cdots & c_{U-2L} \\ c_{U+1} & c_U & c_{U-1} & \cdots & c_{U-2L+1} \\ \vdots & \vdots & \vdots & \cdots & \vdots \\ c_{U+2L-1} & c_{U+2L-2} & c_{U+2L-3} & \cdots & c_{U-1} \\ c_{U+2L} & c_{U+2L-1} & c_{U+2L-2} & \cdots & c_U \end{pmatrix} \cdot \begin{pmatrix} b_{U-L} \\ b_{U-L+1} \\ \vdots \\ b_{U+L-1} \\ b_{U+L} \end{pmatrix} = - \begin{pmatrix} c_{2U-L} \\ c_{2U-L+1} \\ \vdots \\ c_{2U+L-1} \\ c_{2U+L} \end{pmatrix}. \tag{41}$$

Thus, a_i coefficients may be calculated as follows:

$$\begin{pmatrix} a_{U-L} \\ a_{U-L+1} \\ \vdots \\ a_{U+L-1} \\ a_{U+L} \end{pmatrix} = \begin{pmatrix} c_{U-L} & 1 & 0 & \cdots & 0 \\ c_{U-L+1} & c_1 & 1 & \cdots & 0 \\ \vdots & \vdots & \vdots & \cdots & \vdots \\ c_{U+L-1} & c_{2L-1} & c_{2L-2} & \cdots & 0 \\ c_{U+L} & c_{2L} & c_{2L-1} & \cdots & 1 \end{pmatrix} \cdot \begin{pmatrix} 1 \\ b_{U-L} \\ \vdots \\ b_{U+L-1} \\ b_{U+L} \end{pmatrix}. \tag{42}$$

Accordingly, only the first, second, and third subsequences of the autocorrelation sequence are necessary to calculate all parameters, which are

$$[\sigma^2_{\mathrm{AR}}, \gamma_x(\nu), a_{U-L}, \cdots, a_{U+L}, b_{U-L}, \cdots, b_{U+L}].$$

This condition leads to $N \ge 2U + L$ and $P_L \ge 2U + L$ (see Fig. 4). To conclude, the

$$[\sigma^2_{\mathrm{AR}}, \gamma_x(\nu), a_{U-L}, \cdots, a_{U+L}, b_{U-L}, \cdots, b_{U+L}]$$

calculated parameters allows $\alpha(f)$, $\beta(f)$, and $\rho(f)$ parameters estimation so that one is able to find out noise behaviors of the DUT with knowledge of the S-parameters. Furthermore, a way to verify the method capabilities is to compare S_{11} extracted by this method with S_{11} provided by the founder.

V. Noise-Wave Sources and Noise-Parameters Extraction

After several extractions for different drain–current values and different input reflection coefficients, we find out that a first order estimate for the b_U value is

$$b_U \approx -\frac{c_{2U}}{c_U} \tag{43}$$

when $\Gamma_1^{[0]}$ is an open load. Equation (43) is derived from (36) where amplitudes of b_i coefficients for $i \ne U$ are mainly close to zero. Equation (43) underlines the existence of a correlation term. Obviously, if the amplitude of the b_U coefficient is nearly zero (much smaller than 0.1), one may presume uncorrelated noise sources for the DUT. The simplified expression for b_U in (43) leads to the $C(\nu)$ first-order value given by

$$C(\nu) \approx -\frac{\gamma_x(\nu)}{\Gamma_1^{[0]}(\nu)\alpha^2(\nu)} \cdot \frac{c_{2U}}{c_U} \tag{44}$$

where $\Gamma_1^{[0]}$ is an open load. Then, the standard noise parameters may be derived from the noise-wave sources to make the comparison easier with other usual extraction methods [10]. Let us introduce Γ_C and $S_{11_{\mathrm{EQ}}}$ which simplify the following standard noise-parameters expression:

$$b_{\mathrm{N1}} = b_{\mathrm{N1_{NC}}} + \Gamma_C \frac{b_{\mathrm{N2}}}{S_{21}} \tag{45}$$

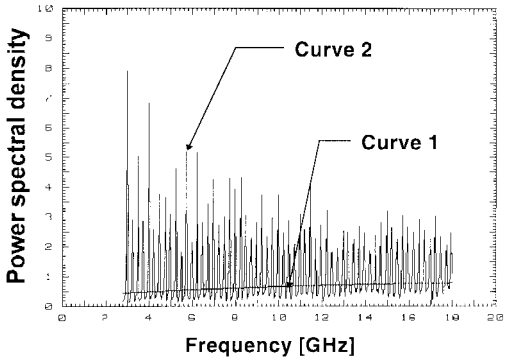

Fig. 5. Curve 1: γ_x extracted value. Curve 2: γ_y measurement.

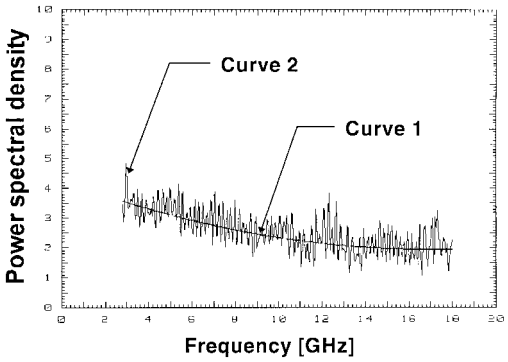

Fig. 6. Curve 1: b_{N2} PSD extracted value. Curve 2: b_{N2} PSD measurement.

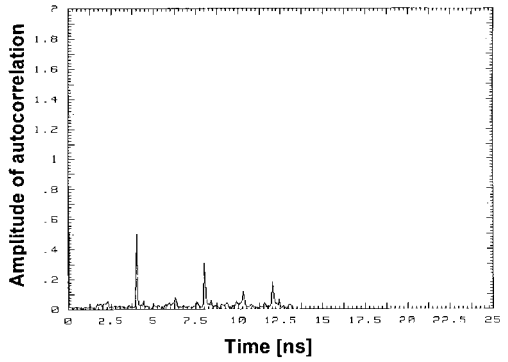

Fig. 7. Autocorrelation function.

where $b_{\mathrm{N1_{NC}}}$ is the part of b_{N1} not correlated with b_{N2}. Now, we are able to define a new reflection coefficient:

$$S_{11_{\mathrm{EQ}}} = S_{11} - \Gamma_C. \tag{46}$$

Then, the standard noise parameters may be written [4], [5] as follows:

Normalized noise resistance:

$$r_n = \frac{1}{4} \cdot \left[\left\langle \left| \frac{b_{\mathrm{N2}}}{S_{21}} \right|^2 \right\rangle \cdot |1 + S_{11_{\mathrm{EQ}}}|^2 + \langle |b_{\mathrm{N1_{NC}}}|^2 \rangle \right]. \tag{47}$$

Optimum reflection coefficient:

$$\frac{\Gamma_{\mathrm{opt}}}{|1+\Gamma_{\mathrm{opt}}|^2} = \frac{S^*_{11_{\mathrm{EQ}}} \langle |b_{\mathrm{N2}}|^2 \rangle}{\langle |b_{\mathrm{N2}}|^2 \rangle \cdot |1 + S_{11_{\mathrm{EQ}}}|^2 + |S_{21}|^2 \langle |b_{\mathrm{N1_{NC}}}|^2 \rangle} \tag{48}$$

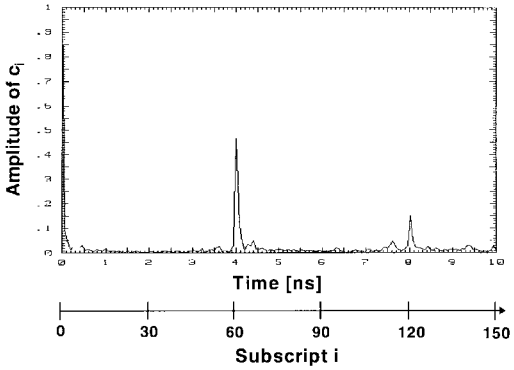

Fig. 8. Amplitude of c_i sequence.

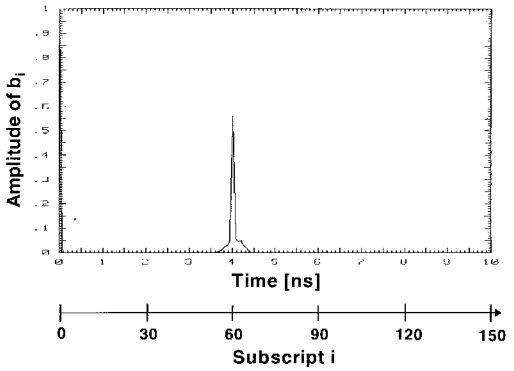

Fig. 9. Amplitude of b_i sequence.

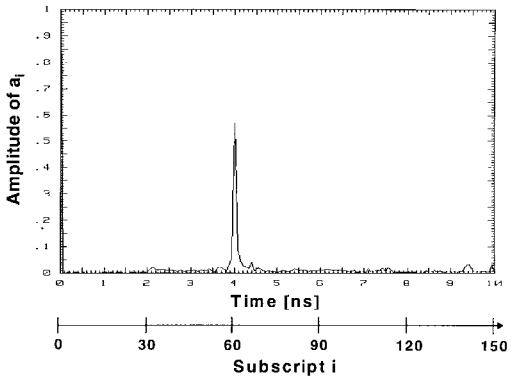

Fig. 10. Amplitude of a_i sequence.

and, therefore,

$$\mathrm{ARG}\,(\Gamma_{\mathrm{opt}}) = -\mathrm{ARG}\,(S_{11_{\mathrm{EQ}}}). \tag{49}$$

Minimum noise factor:

$$F_{\min} = 1 + \left\langle \left| \frac{b_{\mathrm{N2}}}{S_{21}} \right|^2 \right\rangle \cdot [1 - |S_{11_{\mathrm{EQ}}}|\,|\Gamma_{\mathrm{opt}}|]. \tag{50}$$

$|\Gamma_{\mathrm{opt}}|$ values should be derived from (48) by solving a second-degree equation.

VI. Results and Comparisons

The measurements are made in a 2.8–18-GHz frequency range with a 38-MHz frequency step; in this case, a GEC-MARCONI 4 × 75 μm transistor at $V_{\mathrm{gs}} = -0.7$ V, $V_{\mathrm{ds}} = 5$

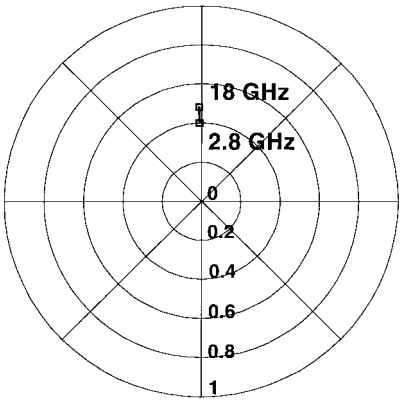

Fig. 11. $\langle b_{\mathrm{N}1} b_{\mathrm{N}2}^{*} \rangle$ extracted value from 2.8 to 18 GHz.

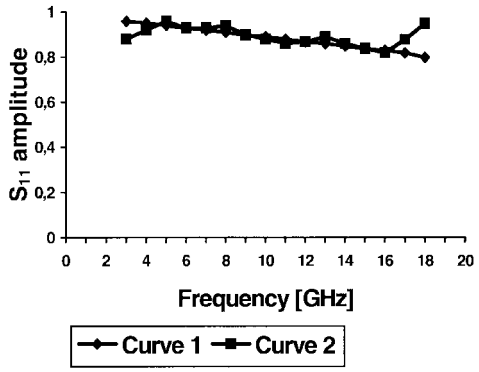

Fig. 12. Comparison between extracted amplitude of S_{11} and S_{11} amplitude given by the founder.

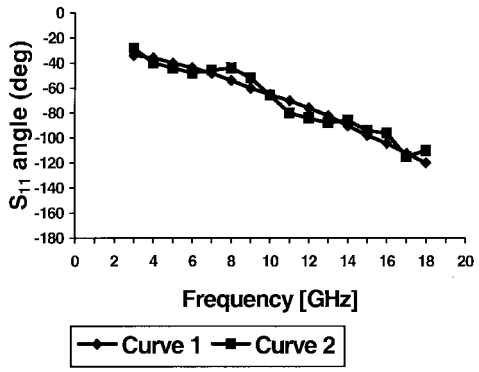

Fig. 13. Comparison between extracted angle of S_{11} and S_{11} angle given by the founder.

V, and $I_{\mathrm{ds}} = 10$ mA. Fig. 5 gives $\gamma_y(f)$ and $\gamma_x(f)$ value for an open load while Fig. 6 indicates $b_{\mathrm{N}2}$ PSD which is fitted by an AR modeling as well. Fig. 7 shows the autocorrelation function obtain by an inverse FT and we find out that τ is approximately 4 ns, corresponding to $U = 61$. Fig. 8 gives the amplitude of c_i coefficients where the first and second scale on X-axis shows the equivalence between the subscript i and the time variable. σ_{AR}^2 parameter is approximately 1.02. Fig. 9 reports the amplitude of b_i coefficients while Fig. 10 shows amplitude of a_i coefficients. Furthermore, Fig. 11 gives $\langle b_{\mathrm{N}1} b_{\mathrm{N}2}^{*} \rangle$ extracted value calculated with relation in (44) and Figs. 12 and 13 reports, on the one hand, the extracted

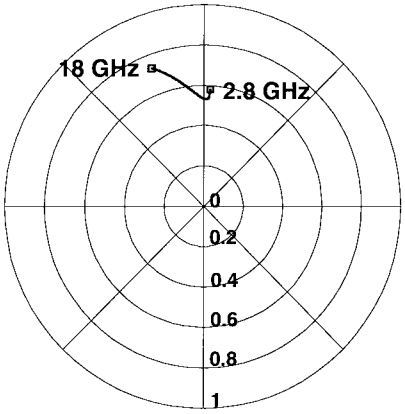

Fig. 14. Representation of correlation coefficient C_{in}.

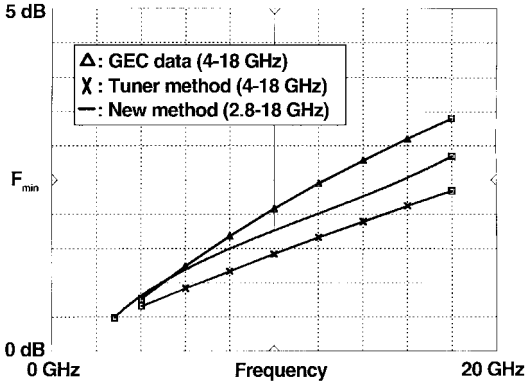

Fig. 15. F_{min} comparison.

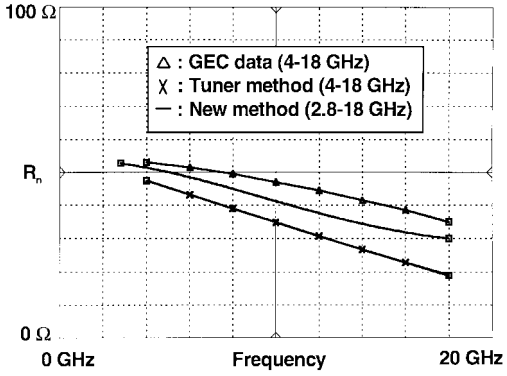

Fig. 16. R_n comparison.

S_{11} reflection coefficient of the transistor (curve 2) and, on the other hand, S_{11} simulated from small-signal parameters (curve 1). Corresponding $C_{\mathrm{in}} = \langle i_g i_d^{*} \rangle / \sqrt{\langle |i_g|^2 \rangle \langle |i_d|^2 \rangle}$ [3] value calculated with these results is mainly imaginary, as shown in Fig. 14, respecting [8]. After this extraction, the calculation of the $b_{\mathrm{N}1}$ PSD value with the acknowledgment of the b_E PSD becomes easy. Finally, comparisons are made with standard noise parameters given by GEC-MARCONI and those measured by a laboratory (Figs. 15–17).

VII. Conclusions

The noise-wave representation offers an alternative analysis which allows time-domain representation of distributed variables. Algorithms derived from spectral parametric modeling

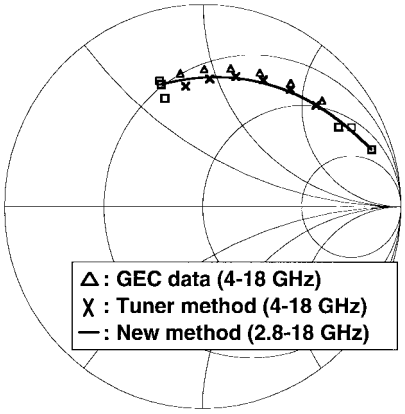

Fig. 17. $\Gamma_{\rm opt}$ comparison.

could be easily implemented on a computer. They could also be implemented on a digital signal processor taking place in the NR. Besides, the method proposed here uses a light setup, requires no source–pull tuner and offers advantages (less time consuming, etc.) over conventional methods. This method will be improved to obtain more accurate noise-source extraction and is promising for millimeter-wave applications.

REFERENCES

[1] J. Max, *Méthodes et techniques de traitement du signal et applications aux mesures physiques* (Books 1 and 2). Paris, France: Masson, 1987.
[2] H. Rohde and W. Dahlke, "Theory of noisy fourpoles," *Proc. IRE*, vol. 44, pp. 811–818, June 1956.
[3] K. Hartmann, "Noise characterization of linear circuits," *IEEE Trans. Circuits Syst.*, vol. CAS-23, pp. 581–590, Oct. 1976.
[4] R. P. Hecken, "Analysis of linear noisy two-ports using scattering waves," *IEEE Trans. Microwave Theory Tech.*, vol. MTT-29, pp. 997–1004, Oct. 1981.
[5] S. W. Wedge and D. B. Rutledge, "Wave techniques for noise modeling and measurement," *IEEE Trans. Microwave Theory Tech.*, vol. 40, pp. 2004–2012, Nov. 1992.
[6] A. Boudiaf, "Development of an automatic noise figure measurement bench at microwave frequencies, noise characterization and modeling of field effect transistors," Ph.D. dissertation, Dept. Inst. d'Electronique Fondamentale, Univ. Paris-Sud, Paris, France, 1993.
[7] S. L. Marple, Jr., *Digital Spectral Analysis with Applications* (Prentice-Hall Signal Processing Series), A. V. Oppenheim, Series Ed. Englewood Cliffs, NJ: Prentice-Hall, 1987.
[8] G. Dambrine, H. Happy, F. Danneville, and A. Cappy, "A new method for on wafer noise measurement," *IEEE Trans. Microwave Theory Tech.*, vol. 41, pp. 375–381, Mar. 1993.
[9] J. Chen, C. Wu, T. K. Y. Lo, K.-L. Wu, and J. Litva, "Using linear and nonlinear predictors to improve the computational efficiency of FD-TD algorithm," *IEEE Trans. Microwave Theory Tech.*, vol. 42, pp. 1992–1997, Oct. 1994.
[10] A. Cappy, "Noise modeling and measurement techniques," *IEEE Trans. Microwave Theory Tech.*, vol. 36, pp. 1–10, Jan. 1988.
[11] C. Eswarappa and W. J. R. Hoefer, "Autoregressive (AR) and autoregressive moving average (ARMA) spectral estimation techniques for faster TLM analysis of microwave structures," *IEEE Trans. Microwave Theory Tech.*, vol. 42, pp. 2407–2411, Dec. 1994.
[12] D. Pasquet, J. R. Riviére, A. Boudiaf, T. Werling, and B. Delacressonniére, "Mesure du facteur de bruit par la méthode des deux températures," in *Ann. des Télécommunications*, pp. 602–610, Dec. 1996.
[13] A. Papoulis, *Probability, Random Variables, and Stochastic Processes*, 3rd ed. New York: McGraw-Hill, 1984.
[14] S. M. Kay, *Modern Spectral Estimation.* New York: Prentice-Hall, 1988.

Thierry Werling (S'97) was born in Strasbourg, France, in 1966. He received the Engineer degree from the Ecole Nationale Supérieure de l'Electronique et de ses Applications (ENSEA), Cergy Cedex, France, in 1992, and the Ph.D. degree in electrical engineering from Paris-Sud University, Orsay, France, in 1997.

He is currently with ENSEA-EMO (one of ENSEA research groups), Cergy Cedex, France. His research interests are noise-measurement techniques, noise-wave analysis, and time-domain analysis.

Emmanuelle Bourdel was born in Paris, France, in 1961. She received the Ph.D. degree from the Institut National des Sciences Appliquées (INSA), Toulouse, France, in 1989.

She is currently an Assistant Professor at the Ecole Nationale Supérieure de l'Electronique et de ses Applications (ENSEA), Cergy Cedex, France, with ENSEA-EMO (the ENSEA microwave laboratory). Her interests are microwave measurements and propagation in planar transmission lines.

Daniel Pasquet (M'86–SM'96) was born in Aulnay-sous-bois, France, in 1948. He received the diploma degree from ENREA (now ENSEA), Cergy Cedex, France, in 1970, the Doctorate degree (thèse de troisième cycle), from Universitè des Sciences et Techniques, Lille, France, in 1975, and the Thèse d'Etat degree from Paris-Sud University, Orsay, France, in 1985.

From 1971 to 1981, he taught at the Institut Universitaire de Technologie (IUT), Calais, France. Since 1981, he has been at the Ecole Nationale Supérieure de l'Electronique et de ses Applications (ENSEA), Cergy Cedex, France, where he became a Professor in 1987.

Dr. Pasquet is the secretary of the French Chapter of the IEEE Microwave Theory and Techniques and IEEE Electron Devices Societies.

Ali Boudiaf was born in Algiers, Algeria, in 1963. He received the Diploma degree in electronics engineering from Polytechnique, Algiers, Algeria, in 1987, and the Ph.D. degree in microelectronics and microwave systems from the University of Paris XI, Orsay, France, in 1993.

From 1989 to 1993, he worked at the Centre National d'Etudes des Télécommunications, Bagneux Laboratory, France, where he was engaged in noise-parameter measurements and modeling of field-effect transistors on GaAs. In 1993, he was been an Assistant Professor at the Ecole Nationale Supérieure de l'Electronique et de ses Applications (ENSEA), Cergy Cedex, France, in 1993. Since 1994, he has been an Assistant Professor at the University of Marne-la-Vallée, Noisy-le Grand Cedex, France. His current interests are new techniques for measuring FET and HBT noise parameters and extracting their models, and the design of low phase-noise MMIC VCO's.